Methods and Supplementary Material

SM1: Materials and Methods

Tubulin was isolated from rat brain as described previously (1) and stored in liquid nitrogen until use. All experiments here utilized PM buffer: 0.1 M Pipes, 1 mM MgCl2, pH 7.0. Assembly of tubulin to Taxol-stabilized microtubules was performed by supplementing a 10 μM tubulin solution in PM buffer with 1 mM GTP followed by 4 μM Taxol, then an additional 16 μM Taxol, with 5 minutes at 37 °C in between each addition. Samples were then incubated at room temperature for 45 minutes. Assembly of tubulin to GMPCPP-stabilized microtubules was performed by supplementing a 10 μM tubulin solution in PM buffer with 0.5 mM GMPCPP and incubating at 37 °C for 30 minutes. Subtilisin digestion was performed according to (7,8).

Microtubules were polymerized in presence of guanosine-5'-[(α,β)-methyleno]triphosphate (GMPCPP) or Taxol, as indicated, before deposition on 200-square mesh copper grids, covered with carbon-only or formvar-carbon films. Grids were floated on ~10 □l solution containing 1 mg/ml of microtubules. The excess was wicked away after ~20 seconds.

An intermediate step was performed before negative staining the microtubules with Methylamine Tungstate (NanoW, Nanoprobe), used as supplied (2% w/v at pH 6.8). Microtubule stabilization was first performed by applying Uranyl Acetate (UA) as described below, resulting in stable samples under the sustained irradiation intrinsic to this imaging protocol. All results shown here have been obtained on stabilized microtubules fixed with UA before further negative staining, as described below.

Staining protocol: ~10 □l drop of UA solution 1% w/v was left in contact with freshly deposited microtubules wicking the excess after ~10 seconds. Successively the grid was washed with distilled water very quickly and negative stained with NanoW. Alternatively, application of NanoW was done with two drops, the first one left in contact with the sample for ~3 seconds, wicking excess, and floating grid on the second one for ~1 minute. Excess was wicked off

again before drying in air for at least 2 minutes, before storing the grids vertically prior to microscopy. Imaging was realized usually within one week from the sample deposition.

Fiduciary markers: depending on the magnification used, 3, or 5 nm gold beads were chosen. In Figure 1 colloidal 5 nm gold spheres were used as fiduciary markers. They were deposited on the surface and allowed to dry before depositing the microtubules, as described above.

Microtubules imaged after digestion with subtilisin were first stabilized with Taxol and then digested overnight before staining as described. Controls were Taxol microtubules left overnight at 37ºC in incubator without subtilisin.

SM2: <u>Electron Microscopy Tomography.</u>

Experiments were carried out with a Tecnai TEM electron microscope operating at 200 keV when available, otherwise routinely with a Jeol TEM electron microscopes operating at 120 keV. Microscopes were equipped with a LaB6 source. No differences regarding rearrangement of stain under irradiation were observed operating routinely at all acceleration voltages listed above and at a magnification leading directly a pixel size from ~1 to 0.21 nm. Stability was tested until 100 keV acceleration voltages, and stain rearrangements were never observed. We speculate that this behavior is a consequence of the fact that tungstate ions are in a stable closed-shell configuration, and the Uranyl ions remained on the sample are stably chemically coordinated by the numerous Lewis-bases on the surface of proteins [1, 2]. Detectors were routinely operated in ‘counting mode’ for all experiments, i.e. actual counts recorded in each pixel were directly proportional to the number of electrons generating the signal. Poisson statistics could therefore be used to assess accuracy of each voxel. This characteristic of the signal has not been fully exploited in this work, although it facilitates exams of direct images and of reconstructed volumes, when the error propagation is done correctly.

Microtubules digested with subtilisin were imaged at 120 keV with a Jeol microscope operated with a LaB6 source. After verification as described, images

were obtained at a magnification leading directly a pixel size of 0.21 nm or higher. The other microtubules here reported were stabilized with GMPCPP and imaged at 200 keV, at a magnification leading directly a pixel size of 0.39 nm. No differences have been noted for the purposes of this work between Taxol- and GMCPP-stabilized microtubules.

In order to achieve high-enough resolution the experimental geometry chosen was uni-axial (as usual in material science experiments), with 1º angular step between images, for a total of 143 images in each experiment [3, 4], in order to satisfy the criterion of enough information content in a tomogram to achieve the desired resolution [5]. The objective aperture of the electron microscopes was either removed or larger than 100 □m diameter in all experiments here reported. Further experiments are underway to assess the actual limit for accessing information of molecular dimensions. The most stringent limitation here seems to be the resolving power of the microscope used, that depends on the wavelength of the radiation (120 or 200 keV) with this contrast method.

The explicit choice done in this work has been to use mainly amplitude scattering (i.e. the real part of the scattering wave function) as the source of image contrast. This choice enables us to use the straight approach (introduced by Abbe and Rayleigh in the last two centuries) for calculating image resolution, provided that enough signal-to-noise (S/N) distinguishes values measured by two neighboring pixels in the image.

For all practical purposes in optical microscopy this translates in considering the theoretical resolution as half the wavelength of the radiation. Since in these experiments the wavelength of accelerated electrons is a few picometers, the theoretical resolution of an electron microscope accelerating the electrons to 200 keV is only limited by electro-optical aberrations to 0.2 nm [9].

The calculated virtual sections shown here would have actually an increased resolution with respect to the initial images, acquired at 0.37 nm pixel size. This increase is thought to be inversely proportional to the number of images combined in order to calculate the virtual sections in the tomogram [5].

In order not to oversample, and considering the grain size of the stain, images

have been acquired slightly above the tabulated power of resolution of the microscope used. The pixel size chosen was 0.37 nm (at 200 keV) or ~0.25 nm (at 120 keV). The reader should consider that, in the conditions of the experiment, a small amount of electrons may be scattered at angles such that the signal will be recorded in the pixels neighboring where the scattering phenomenon occurred.

Considering these factors, but because we recorded the images using an electron dose allowing to distinguish the intensity in adjacent pixels (since the EM signal is acquired in Poissonian statistics), we think reasonable to conclude that all images reported in this article, and therefore also all corresponding renderings, have a resolution of at least two pixel sizes, i.e. ~0.7 nm. This result has been obtained from one experiment done in one day, with the successive elaboration done in a few hours, after optimizing the sample preparation protocol and the microscope alignment.

Experiments were conducted using a high-tilt Gatan holder bi-axial, although a mono-axial acquisition protocol was chosen. Experiments were routinely set between $\pm$71º, recording an image every 1º of rotation, setting the acquisition software (SERIALEM) for counting at least 5000 e^-/nm^2 per image. Therefore the total electron dose intrinsic to an experiment was of the order of 10^6 e^-/nm^2, since the beam was not obscured during movements of the stage.

Raw images as function of angle between the electron beam and the sample have been aligned using cross correlation spatial procedures and fiduciary markers of appropriate size. Fiduciary markers diameter was chosen to be roughly 15 pixels diameter at least.

Aligning of the raw images and centering has been implemented using the ETOMO/IMOD shareware package [6] of the university of Boulder, (CO). This packet has been used with all default parameters, besides indicating that fiduciary markers were only on one side during their alignment. Before the calculation of the tomogram the aligned image stack from ETOMO has been corrected with the routine DENSNORM (included in the package). Such correction takes into account the extra weakening of the signal at low surface

angles in view of the thick slab of stained material which the radiation has to penetrate before reaching the detector. Instead, it still has to be implemented a precise calculation of the error bars at the highest values of height (z) in the reconstructed volume, which depends on the fact that a higher number of projections are used for calculating the most external voxels of the microtubules (in our specific application). This fact generated the choice of focusing on the information contained in the most external protofilaments of two microtubules in Fig. 5, in order to put in evidence the effect of Subtilisin only on one microtubule.

After aligning the raw images, the ETOMO package was also used to calculate corresponding tomograms both with the back-projection method and with SIRT. No major differences between virtual sections arising from these two methods of calculation have been observed. Nevertheless, when not otherwise specified, all results shown come from 30 iterations using SIRT.

Tomogram output has been routinely polished using Gaussian blur spatial filter of Full-Width-Half-Maximum (FWHM) ~0.8 up to ~1.5 pixels. This choice has been dictated by the need of not inserting unwanted information in the tomogram of the order of a few pixel sizes. Rendering of tomograms has been realized imposing a constant threshold to the whole dataset displayed with Chimera (shareware software from UCSF).

Supplementary Pictures

Figure S1

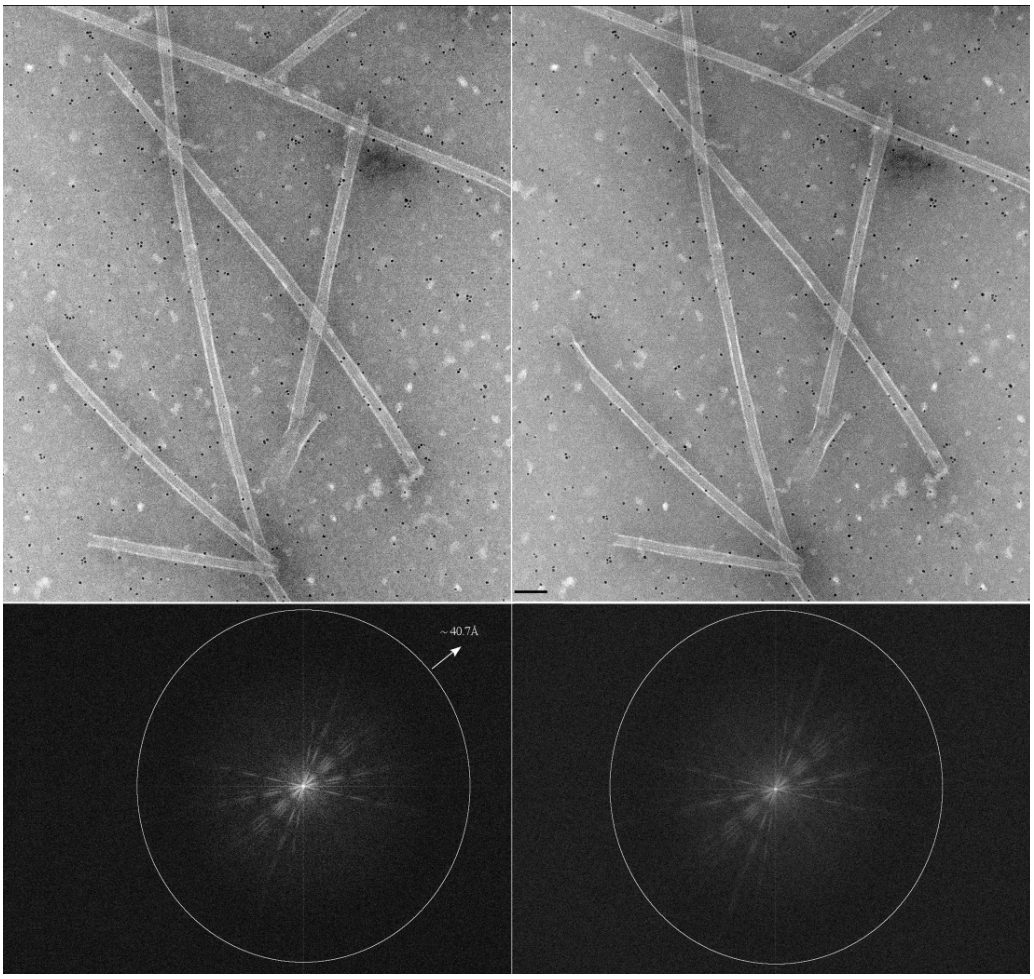

Microtubules imaged after negative staining as explained, just before (a) and immediately after (b) collection of a tomography series of 143 images. Comparison of corresponding Fast Fourier Transforms (below) demonstrate no rearrangements of the stain detected (last part not shown for clarity). Small differences between images seem due to variations of the beam, since here focus level was not fixed by software. White circles represent ~40.7Å in both pictures. Constant periodic arrangement of tubulin subunits in linear arrangements is apparent. Gold fiduciary markers: 5 nm. Scale bar: 50 nm.

Figure S2

Analysis under continuous illumination of the behavior of a sample prepared in the same way as described. Taxol stabilized microtubules stained in the way described were deposited on a formvar-carbon coated 200 mesh (from Electron Microscopy Sciences, EMS) copper grid together with 3 nm colloidal gold. Representative microtubules (Fig S2-A) were illuminated continuously for over 1 hour. For clarity, the area inside the yellow rectangle is shown at the beginning (Fig. S2-B) and after 60 minutes continuous illumination (Fig. S2-C). Focusing has been modified during the experiment. The Gatan detector was operated in counting mode such that counts are directly proportional to electrons. The unsigned 16-bits integers had lower values in the picture acquired after 60 minutes continuous illumination. The difference was a uniformly black image with values corresponding to zero electrons within 3% experimental errors.

S2-A

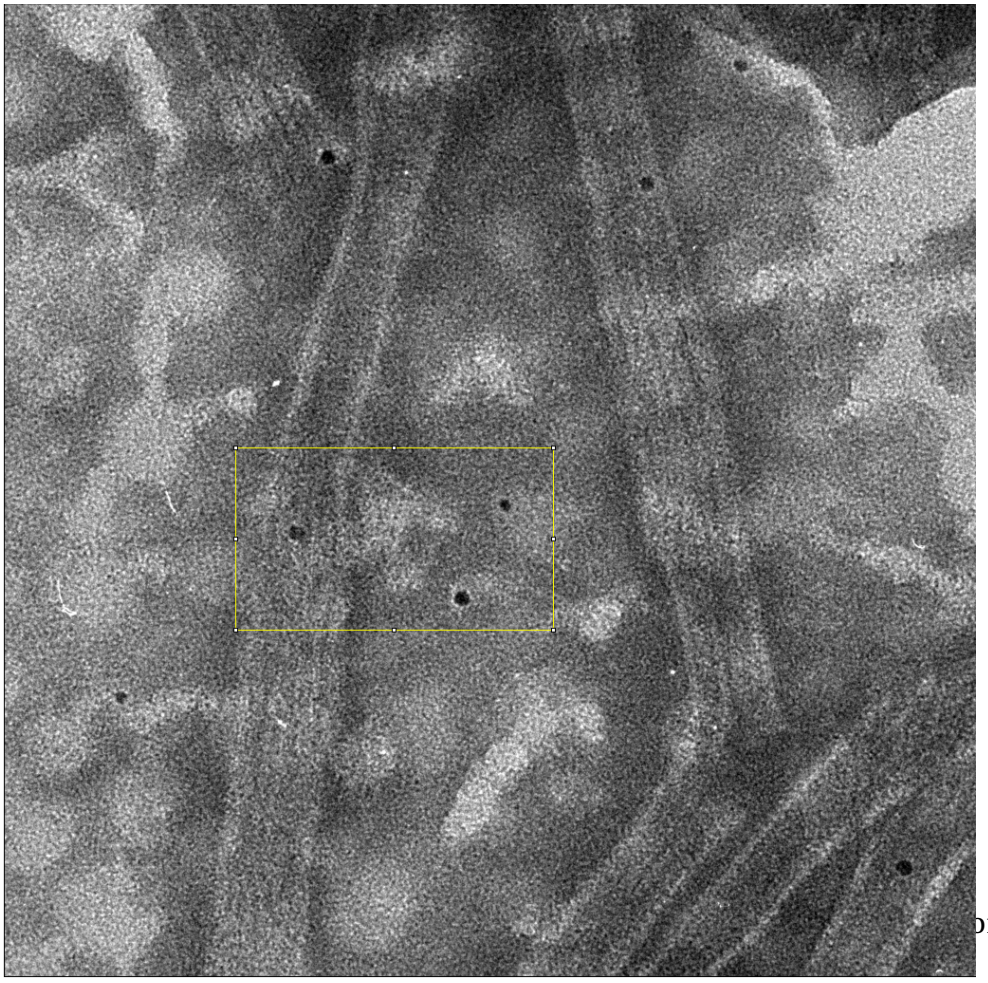

S2-B

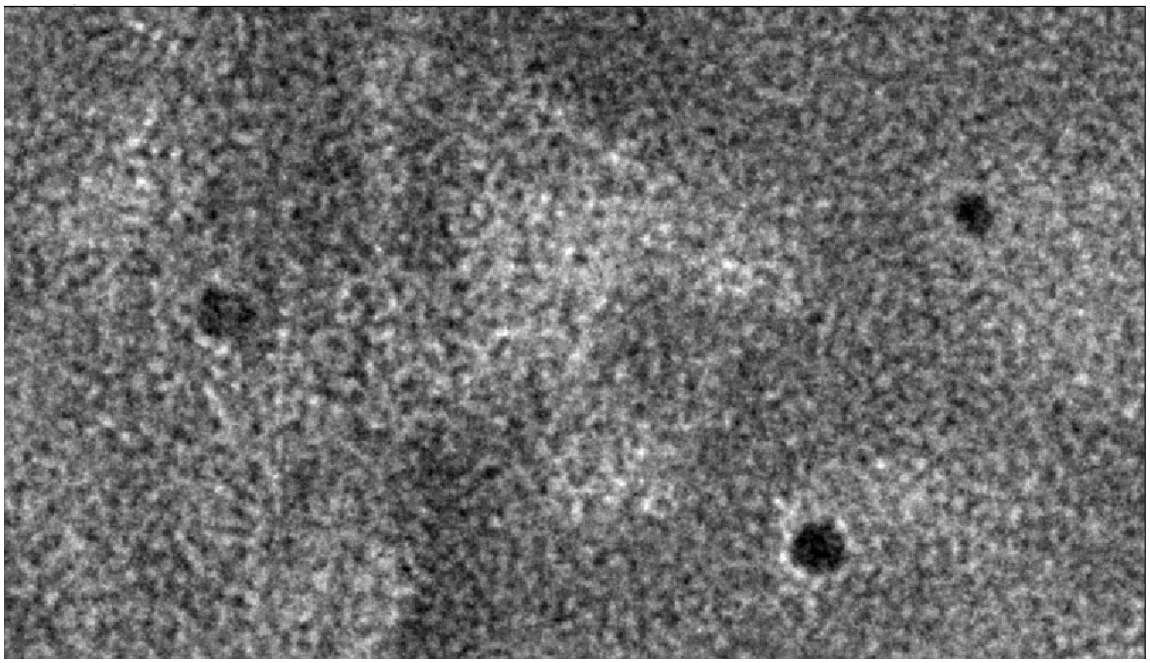

S2-C

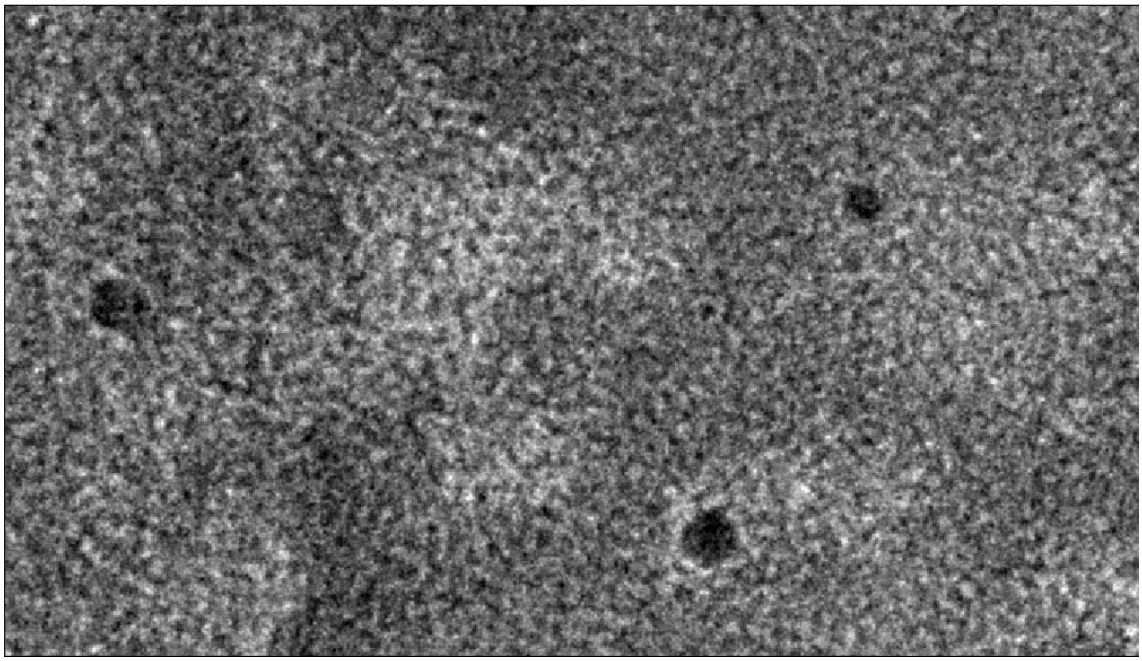

Figure S3

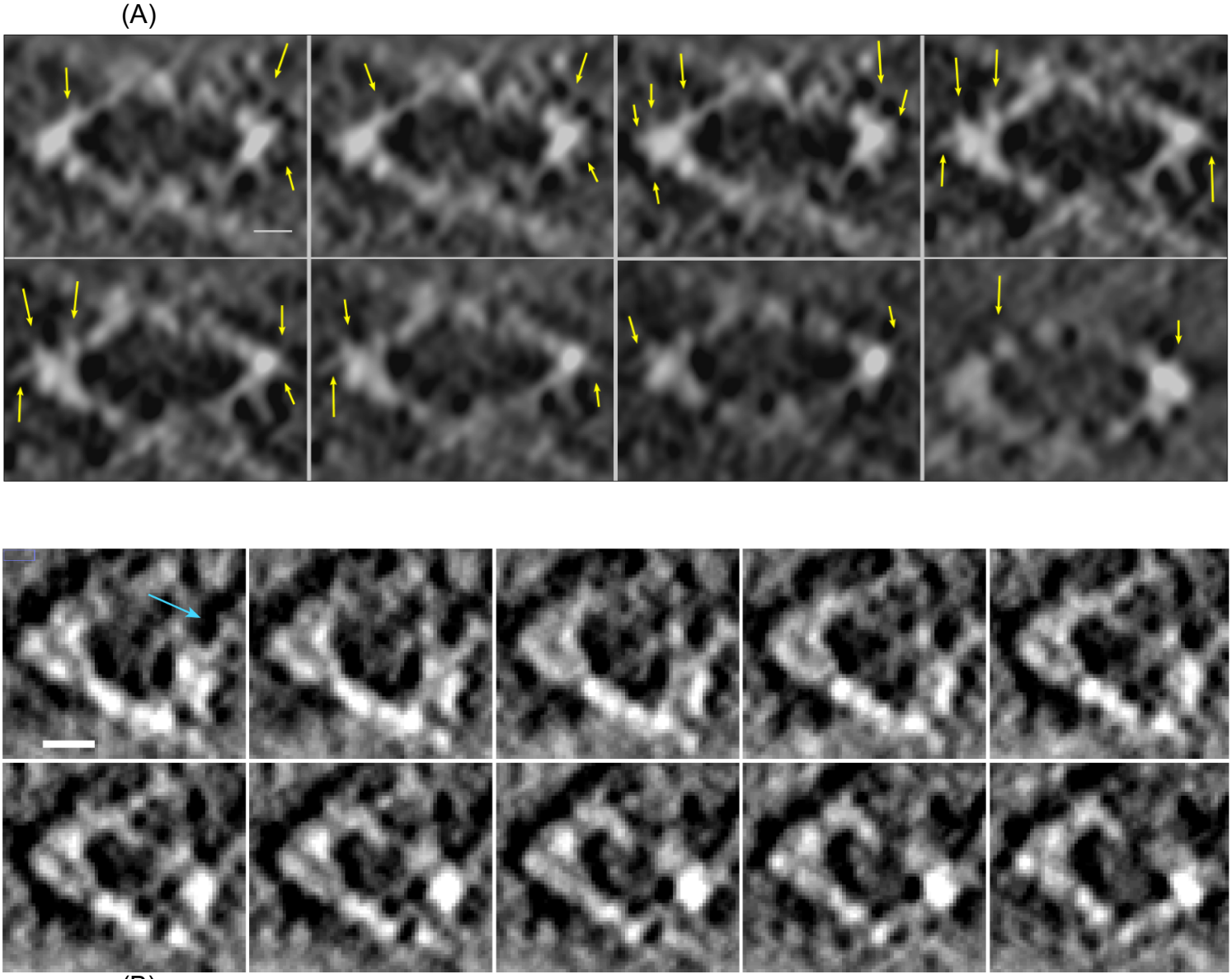

Cross sectional virtual sections perpendicular to the long axis of a microtubule (as in Fig. 4). (A) GMPCPP– and (B) Taxol–stabilized microtubule after cleavage with Subtilisin (see text). Top panel reports virtual sections from same experiment in Fig 1 and 4A. Virtual sections are chosen of arbitrary numbers 1, 2, 3, 7, 8, 9, 11, 311 along the long axis of the microtubule relative to an arbitrary start at virtual section 1. Because of the small thickness of the sections (0.39 nm)

it is possible to choose one very far (311 sections corresponding to ~120 nm) in the XY plane. This choice is justified to document that this behavior is not a function of the place chosen. Examples are chosen here to be a collection of consecutive and non-consecutive sections. Yellow lines in A indicate possible C-terminals.

(B) panel is obtained from a microtubule polymerized and digested overnight with Subtilisin. These virtual sections are all consecutive and acquired at a magnification leading directly a pixel size ~0.25 nm. Light blue arrow (top left) indicate the attachment of a sheet of tubulin contiguous to this microtubule, as previously found for Subtilisin-digested microtubules [7, 8].

Scale bar: 10 nm.

References

1. F.P. Ballistreri, G.L., A. Pappalardo, F. Punzo, A. Thompson, G.A. Tomaselli, R.M. Toscano, G. Trusso Sfrazzetto, *An integrated X-ray and molecular dynamics study of uranyl–salen structures and properties.* Dalton Trans, 2012. **41**: p. 1951-1960.
2. G. Brancatelli, S.G., A. Notti, A. Pappalardo, G. Trusso Sfrazzetto, *Mono and dinuclear uranyl(VI) complexes with chiral Schiff base ligand.* Inorg. Chimica Acta, 2013. **396**: p. 25-29.
3. A. Fera, J.E.F., J Zimmerberg, T S Reese, *A Negative Stain for Electron Microscopic Tomography.* Microscopy and Microanalysis, 2012. **18**: p. 1–5.
4. Fera A, D.A., Sousa AA, Yang C, Leapman RD, Reese TS., *Direct visualization of CaMKII at postsynaptic densities by electron microscopy tomography.* J Comp Neurol., 2012. **15**: p. 4218-25.
5. KLUG, D.J.D.R.A., *Reconstruction of Three Dimensional Structures from Electron Micrographs.* Nature, 1968. **217**: p. 130-134.
6. Kremer J.R., D.N.M.a.J.R.M., *Computer visualization of three-dimensional image data using IMOD.* J. Struct. Biol, 1996. **116**: p. 71-76.
7. Sackett, D.L., B. Bhattacharyya, and J. Wolff, *Tubulin Subunit Carboxyl Termini Determine Polymerization Efficiency.* Journal of Biological Chemistry, 1985. **260**(1): p. 43-45.
8. Sackett, D.L. and J. Wolff, *Proteolysis of Tubulin and the Substructure of the Tubulin Dimer.* Journal of Biological Chemistry, 1986. **261**(19): p. 9070-9076.
9. David Smith, *Ultimate Reslution in the Electron Microscope?,* Materials Today – Microscopy ; Special Issue, pp 30-38, ISSN:1369 7021 © Elsevier Ltd 2008